INTERNATIONAL JOURNAL FOR NUMERICAL METHODS IN FLUIDS, VOL. 25, 105–121 (1997)

SPIKES AND JITTERING IN THE NUMERICAL SOLUTION OF THE PLANETARY BOUNDARY LAYER PROBLEM: CAUSES AND EFFECTS

A. G. PUFAHL[1]*, B. A. KAGAN[2] AND W. EIFLER[1]

[1]*Joint Research Centre of the CEC, IRSASAI, TP 690, I-21020 Ispra, VA, Italy*
[2]*P. P. Shirshov Institute of Oceanology, Russian Academy of Sciences, St. Petersburg, Russia*

SUMMARY

Numerical experiments performed with all possible combinations of approximations for the equations of a one-dimensional planetary boundary layer model employing a one-equation turbulence closure scheme and a staggered, homogeneous, finite difference grid show that spikes and jittering in the vertical profiles of predicted variables are caused by an inappropriate numerical description of the turbulent kinetic energy equation. Jittering arises when using both moderate and large time steps, while spikes occur for large time steps only. There exist two types of jittering: transient and permanent. The former has a lifetime of about 1 week and occurs with large time steps. Permanent jittering, on the other hand, is observed when using moderate time steps and has a lifetime of more than a 1000 days. Introducing an iterative procedure for the eddy viscosity eliminates spikes and permanent jittering but is unsuccessful in removing transient jittering. It is further found that the transition to instability of the solution can be either a sudden or a gradual one. In the case of a sudden transition no numerical peculiarities are observed, whereas for a gradual transition to instability, jittering is present during the entire transition period. In this sense, jittering may be regarded as a herald of instability. Finally, a combination which employs implicit approximations consistently for all the terms in the model equations, regardless of whether using an implicit or semi-implicit approximation for the Coriolis term, proves to be devoid of any numerical artefacts without the need for introducing the iterative procedure for the eddy viscosity.

Int. J. Numer. Meth. Fluids, **25**: 105–121 (1997).

No. of Figures: 5. No. of Tables: 0. No. of References: 15.

KEY WORDS: finite difference approximation; planetary boundary layer problem; spikes; jittering

1. INTRODUCTION

Numerical solutions to the turbulent planetary boundary layer problem are often accompanied by the appearance of specific phenomena known as spikes and jittering. Here spikes are defined as drastic changes in the turbulence characteristics associated with step-like features in the vertical mean velocity profiles which occur in the vicinity of the outer boundary of either the upper or the bottom

* Correspondence to: A. G. Pufahl, Joint Research Centre of the CEC, IRSASAI, TP 690, I-21020 Ispra, VA, Italy

Contract grant sponsor: European Community/Human Mobility and Capital

CCC 0271–2091/97/010105–17 $17.50

Received February 1996
Revised September 1996

boundary layer. Jittering consists of a zigzag-like change in the predicted profiles of the turbulence and mean flow characteristics observable throughout the entire boundary layer thickness. Without any doubt, 'a jittering eddy viscosity profile with a maximum value of 15,000 $cm^2\ s^{-1}$', which has been observed by Frey,[1] should be considered an unphysical feature. Observations of this kind were made by several authors who described this peculiar behaviour as 'unacceptable oscillations', 'unphysical noise' and 'unrealistic profiles'.

Let us recall precisely what it was they discovered leading to these interpretations. Frey[1] reported rather high values and jittering profiles of eddy viscosity and diffusivity coefficients and step-like profiles of scalar characteristics, employing a modified version of the Mellor–Yamada level 2 closure scheme (a description of the Mellor–Yamada hierarchy of turbulence closure schemes can be found in References 2 and 3). Davies and Jones[4] detected significant time step oscillations of current velocity in the near-bed layer and evidence of this was found in the upper part of the boundary layer. The modulus of the bottom shear stress showed severe time step oscillations which eventually corrupted the solution. Instantaneous vertical profiles of shear stress also showed significant oscillations, having maximum amplitudes close to the base of the boundary layer. These results were obtained by using various versions of a one-equation turbulence model (for a detailed classification of turbulence models see e.g. References 5–7). Deleersnijder and Luyten,[8] in frames of the standard Mellor–Yamada level 2·5 model, obtained profiles of velocity and buoyancy which exhibited such a high level of noise that it was regarded as being unphysical. This noise was associated with large-amplitude oscillations in the profiles of eddy viscosity and diffusivity. Davies *et al.*,[9] using a zero-equation local equilibrium turbulence model with Blackadar's mixing length approximation, mentioned that a strong jittering began to grow at the point where the eddy viscosity decreased and that this jittering was amplified in time. Burchard and Baumert[10] confirmed that both the Mellor–Yamada level 2 model and a local equilibrium turbulence model created oscillating zigzag profiles of eddy viscosity.

Clearly, the above-mentioned symptoms show common features: jittering in the vertical profiles of the turbulence characteristics, mean velocity and scalar quantities when dealing with boundary layer problems. However, even though all authors who observed these features agree that this spurious oscillating behaviour is both unphysical and unacceptable, their explanations of possible causes and how to seek remedies are rather contradictory.

Frey[1] found that jittering occurs whenever a time step $\Delta t > 2(\Delta z)^2/\max(\nu)$ is chosen (here Δz is the vertical grid spacing and ν is the eddy viscosity). He also noticed that two different approximations of the shear production term in the turbulent kinetic energy equation, as suggested by Davies and Jones[4] and Duwe *et al.*,[11] yield stronger jittering in the case of non-constant forcing, but added that this feature was damped out after some time of constant forcing. As possible solutions to the problem of jittering he recommended to choose either a suitably small time step to be estimated by some trial-and-error runs, or an iteration of the eddy viscosity, which, however, did not solve the problem, or to smooth the transition from turbulent to laminar flow by introducing an artificial background viscosity.

Davies and Jones[4] performed calculations using a number of different approximations for the dissipation and shear production terms in a one-equation b–L model, which includes a prognostic equation for the turbulent kinetic energy b and an algebraic expression for the mixing length L. They found that the reason for the emergence or disappearance of oscillations when using one form of approximation of the dissipation and shear production terms or the other was not clear. Introducing a time-filtering procedure or an iterative predictor–corrector scheme for the eddy viscosities did not eliminate the oscillations in all the cases under consideration.

Deleersnijder and Luyten[8] argued that the inappropriate behaviour of the stability function in the Mellor–Yamada level 2·5 model, which involves an expression for the vertical shear stress, was a probable reason for the lack of robustness. They noticed that, via a positive feedback accounted for in

this stability function, an increase in shear stress leads to decreasing eddy viscosities and might eventually result in a discontinuity in the velocity, giving rise to an unphysical source of turbulent kinetic energy. They also pointed out that jittering was not a transient feature and did not seem to be directly related to the grid resolution. As a remedy they proposed to use the so-called 'quasi-equilibrium parametrization', put forward by Galperin *et al.*,[12] but mentioned that using another type of numerical scheme might improve the results of the standard Mellor–Yamada level 2·5 model.

Burchard and Baumert[10] also stated that the time step had to be reduced to avoid these unrealistic zigzag profiles and added that the local equilibrium model seemed to be less sensitive to the choice of the time step than did the Mellor–Yamada level 2 model.

Davies *et al.*[9] carried out a number of numerical experiments confirming the existence of a critical time step, as proposed by Frey,[1] beyond which jittering occurs. They also compared the results of the zero-equation local equilibrium model with a one-equation b–L model, where no jittering was observed, and concluded that the problem of jittering was probably due to neglecting the vertical diffusion term in the turbulent kinetic energy equation, which, although small, might efficiently smooth out oscillations induced by the numerical scheme. Further, they argued that jittering was directly related to the vertical grid spacing and could be avoided when using a fine resolution.

The aim of this report is thus to answer the following questions. What are the causes responsible for these phenomena, i.e. are these features due to the physical assumptions underlying the model or are they purely of numerical origin? How long do these peculiar features persist? What is it necessary to do to eliminate these numerical artefacts?

In order to answer these questions, a one-dimensional model employing a one-equation b–L turbulence closure scheme is considered. Care is taken that the fundamental physical processes controlling the time–space variability of the planetary boundary layer are accounted for. The approximation for the mixing length within the boundary layer follows Blackadar's[13] proposal.

Further, allowance is made for each of the terms in the model equations to be calculated with either an explicit, implicit or semi-implicit approximation, with the exception of the temporal change term which is approximated with a first-order, foward-in-time scheme. All possible combinations of the approximations for the different terms, as well as two different semi-implicit schemes for the shear production term in the turbulent kinetic energy equation, were examined.

As a test case we considered the evolution of a surface neutrally stratified planetary boundary layer forced by a constant wind stress. The appropriate numerical experiments were peformed with six different time steps ranging from 1 h to 30 s on a homogeneous, staggered, finite difference grid with $\Delta z = 1{\cdot}0$ m (unless specified otherwise). It is shown that the phenomena are caused by choosing certain combinations of approximations of the terms in the turbulent kinetic energy equation and that they may be classified as spikes, observable at large time steps only ($\Delta t = 1$ h), and jittering. Jittering can present itself as either a transient feature, observable exclusively at larger time steps and having a lifetime of up to several days, or a permanent feature, observable when using smaller time steps and which persists for more than a 1000 days. Permanent jittering, in turn, can show up in the vertical profiles of either the turbulence characteristics only or both the turbulence characteristics and the mean velocity. It was found that the only way to avoid any of these features is to use implicit approximations consistently for all the terms in the turbulent kinetic energy equation. Introduction of an iterative procedure for the eddy viscosity was found to eliminate spikes and permanent jittering but was not successful in removing transient jittering.

The paper is organized as follows. The model equations with their initial and boundary conditions are presented in the next section. In Section 3 the finite difference approximation of the boundary value problem is discussed in some detail. Section 4 contains a description of the numerical experiments which were performed to understand the causes leading to spikes and jittering and an analysis of these phenomena. The paper ends with Section 5 including the conclusions.

2. PLANETARY BOUNDARY LAYER MODEL

The model equation for momentum in terms of the complex velocity $w = u + \mathrm{i}v$ (here u and v are the x- and the y-component of the current velocity respectively) is written as

$$\frac{\partial w}{\partial t} + \mathrm{i}fw = -\frac{1}{\rho_0}\left(\frac{\partial p}{\partial x} + \mathrm{i}\frac{\partial p}{\partial y}\right) + \frac{\partial}{\partial z}\left(\nu\frac{\partial w}{\partial z}\right). \tag{1}$$

This equation is supplemented with the turbulent kinetic energy equation

$$\frac{\partial b}{\partial t} = \frac{\partial}{\partial z}\left(\alpha_\mathrm{b}\nu\frac{\partial b}{\partial z}\right) + \nu\left|\frac{\partial w}{\partial z}\right|^2 - c_1\frac{b^{3/2}}{L} \tag{2}$$

and the definition of the eddy viscosity coefficient

$$\nu = c_0 L b^{1/2}, \tag{3}$$

where L is the mixing length defined in accordance with Blackadar[13] as

$$L = \frac{\kappa(H - z)}{1 + \kappa(H - z)/L_0}. \tag{4}$$

In these equations, p denotes pressure, which in the following sections is assumed to be horizontally homogeneous, being equivalent to the case of purely wind-driven flow; b is the turbulent kinetic energy; L_0 is the limiting value of the mixing length; f is the Coriolis parameter; ρ_0 is a constant reference density; H is the total water depth; z is the vertical co-ordinate, having its origin at the seabed and increasing upwards; t is time; κ is von Karman's constant; α_b is the ratio of the eddy diffusivity to the eddy viscosity, which for simplicity is taken to be unity; and $c_0 = 0{\cdot}5$ and $c_1 = c_0^3 = 0{\cdot}125$ are numerical constants (see e.g. Reference 14).

The various terms in (1) and (2) are as follows: $\partial w/\partial t$ and $\partial b/\partial t$ are the temporal rates of change; $\mathrm{i}fw$ is the Coriolis term; $\partial(\nu\partial w/\partial z)/\partial z$ and $\partial(\alpha_\mathrm{b}\nu\partial b/\partial z)/\partial z$ are the vertical momentum and turbulent kinetic energy diffusion respectively: $\nu|\partial w/\partial z|^2$ is the shear production and $c_1(b^{3/2}/L)$ the dissipation ε of turbulent kinetic energy.

Equations (1)–(3) form a closed set and are solved subject to some arbitrary initial conditions ($w = w^0$ and $b = b^0$ at $t = 0$) and the boundary conditions

$$w = 0 \quad \text{and} \quad b = (1/c_0^2\rho_0)|\underline{\tau}^\mathrm{b}|^2 \quad \text{at } z = 0, \tag{5}$$

$$\rho_0\nu(\partial w/\partial z) = \underline{\tau}^\mathrm{s} \quad \text{and} \quad b = (1/c_0^2\rho_0)|\underline{\tau}^\mathrm{s}|^2 \quad \text{at } z = H, \tag{6}$$

where $\underline{\tau}^\mathrm{s}$ is the surface wind stress and $\underline{\tau}^\mathrm{b}$ is the bottom shear stress defined as $\underline{\tau}^\mathrm{b} = \rho_0\nu(\partial w/\partial z)$ at $z = 0$. The boundary conditions for b are derived from the condition of local balance of turbulent kinetic energy generation and dissipation and hence are in essence equivalent to the zero-flux condition for turbulent kinetic energy, considering that the turbulent kinetic energy is constant in the near-surface and near-bed layer.

3. FINITE DIFFERENCE APPROXIMATION

Equations (1) and (2) are discretized in the vertical by means of finite differences on a homogeneous, staggered grid. In other words, the velocites are calculated at the grid points with subscript k and all

turbulence characteristics (b, L, v) as well as the vertical mean velocity shear are calculated at intermediate grid points. As a result, Equation (1) is reduced to the form

$$\frac{w_k^{t+1}-w_k^t}{\Delta t}+\mathrm{i}f[\theta_1 w_k^{t+1}+(1-\theta_1)w_k^t]=p^t+\frac{2\theta_2}{\Delta z_{k+1}+\Delta z_k}\left(v_{k+1}\frac{w_{k+1}^{t+1}-w_k^{t+1}}{\Delta z_{k+1}}-v_k\frac{w_k^{t+1}-w_{k-1}^{t+1}}{\Delta z_k}\right)$$
$$+\frac{2(1-\theta_2)}{\Delta z_{k+1}+\Delta z_k}\left(v_{k+1}\frac{w_{k+1}^{t}-w_k^{t}}{\Delta z_{k+1}}-v_k\frac{w_k^{t}-w_{k-1}^{t}}{\Delta z_k}\right), \tag{7}$$

where Δz and Δt are the vertical grid spacing and the time step respectively. It is readily seen that if $\theta=(\theta_1,\theta_2)=0$, we obtain an explicit approximation, if $\theta=1$, an implicit approximation, and if $\theta=\frac{1}{2}$, a semi-implicit approximation for both the Coriolis and vertical diffusion terms.

The temporal rate of change in (2) and the vertical diffusion term are approximated in a similar manner and will not be repeated here. The term describing the production of turbulent kinetic energy due to the vertical mean velocity shear is approximated using two different schemes,[4] namely

$$v\left|\frac{\partial w}{\partial z}\right|^2\approx\theta_3 v_k\left[\left(\frac{u_k^{t+1}-u_{k-1}^{t+1}}{\Delta z_k}\right)^2+\left(\frac{v_k^{t+1}-v_{k-1}^{t+1}}{\Delta z_k}\right)^2\right]+(1-\theta_3)v_k\left[\left(\frac{u_k^{t}-u_{k-1}^{t}}{\Delta z_k}\right)^2+\left(\frac{v_k^{t}-v_{k-1}^{t}}{\Delta z_k}\right)^2\right], \tag{8}$$

$$v\left|\frac{\partial w}{\partial z}\right|^2\approx v_k\left[\left(\theta_3\frac{u_k^{t+1}-u_{k-1}^{t+1}}{\Delta z_k}+(1-\theta_3)\frac{u_k^{t}-u_{k-1}^{t}}{\Delta z_k}\right)^2+\left(\theta_3\frac{v_k^{t+1}-v_{k-1}^{t+1}}{\Delta z_k}+(1-\theta_3)\frac{v_k^{t}-v_{k-1}^{t}}{\Delta z_k}\right)^2\right]. \tag{9}$$

Thus we have an explicit approximation for $\theta_3=0$, an implicit approximation for $\theta_3=1$ and two different semi-implicit approximations for $\theta_3=\frac{1}{2}$, labelled SP1 and SP2:

$$\mathrm{SP1}=\frac{v_k}{2}\left[\left(\frac{u_k^{t+1}-u_{k-1}^{t+1}}{\Delta z_k}\right)^2+\left(\frac{v_k^{t+1}-v_{k-1}^{t+1}}{\Delta z_k}\right)^2\right]+\frac{v_k}{2}\left[\left(\frac{u_k^{t}-u_{k-1}^{t}}{\Delta z_k}\right)^2+\left(\frac{v_k^{t}-v_{k-1}^{t}}{\Delta z_k}\right)^2\right], \tag{10}$$

$$\mathrm{SP2}=\frac{v_k}{4}\left[\left(\frac{u_k^{t+1}-u_{k-1}^{t+1}}{\Delta z_k}+\frac{u_k^{t}-u_{k-1}^{t}}{\Delta z_k}\right)^2+\left(\frac{v_k^{t+1}-v_{k-1}^{t+1}}{\Delta z_k}+\frac{v_k^{t}-v_{k-1}^{t}}{\Delta z_k}\right)^2\right]. \tag{11}$$

The approximation of the dissipation term requires some comment. After eliminating L from the expression for ε by using (3), the dissipation term reads

$$\varepsilon=(c_0^4/v)b^2. \tag{12}$$

The turbulent kinetic energy b appearing in this equation is approximated as

$$b\approx b^t+\theta_4(b^t-b^{t+1}), \tag{13}$$

so that squaring expression (13) yields

$$b^2\approx(b^t)^2+2\theta_4 b^t(b^{t+1}-b^t)+\theta_4^2(b^{t+1}-b^t)^2. \tag{14}$$

If one assumes that $b^{t+1} \to b^t$ when approaching steady state, then the last term on the right-hand side of (14) may be neglected and expression (12) takes the form

$$\varepsilon \approx (c_0^4/v_k)[2\theta_4 b_k^t b_k^{t+1} + (1-2\theta_4)(b_k^t)^2]. \tag{15}$$

Thus we obtain an explicit approximation $\varepsilon \approx (c_0^4/v_k)(b_k^t)^2$ for $\theta_4 = 0$, a semi-implicit approximation $\varepsilon \approx (c_0^4/v_k)(b_k^t b_k^{t+1})$ for $\theta_4 = \frac{1}{2}$ and an implicit approximation $\varepsilon \approx (c_0^4/v_k)[2b_k^t b_k^{t+1} - (b_k^t)^2]$ for $\theta_4 = 1$ (note that for simplicity we call this expression 'implicit' even though it involves partial implicitness only).

The discretized boundary condtions for momentum are

$$\underline{\tau}_{k\mathrm{b}} = \rho_0 v_{k\mathrm{b}} \frac{w_{k\mathrm{b}}}{\Delta z_{k\mathrm{b}}} \equiv \underline{\tau}^{\mathrm{b}} \quad \text{at } z = 0, \qquad \underline{\tau}_{k\mathrm{s}+1} = \rho_0 v_{k\mathrm{s}+1} \frac{w_{k\mathrm{s}+1} - w_{k\mathrm{s}}}{\Delta z_{k\mathrm{s}+1}} \equiv \underline{\tau}^{\mathrm{s}} \quad \text{at } z = H$$

and for turbulent kinetic energy are

$$b_{k\mathrm{b}} = \frac{1}{c_0^2 \rho_0} |\underline{\tau}^{\mathrm{b}}|^2 \quad \text{at } z = 0, \qquad b_{k\mathrm{s}} = \frac{1}{c_0^2 \rho_0} |\underline{\tau}^{\mathrm{s}}|^2 \quad \text{at } z = H.$$

Note that, without using a refined grid in the near-bed region, the implementation of the no-slip condition for momentum, together with the above boundary condition for turbulent kinetic energy, is apparently somewhat unnatural. Instead of employing the no-slip condition, it would be better to specify the equality of the momentum flux to the bottom shear stress, which could be parametrized, for example, by the quadratic resistance law. However, for the case under consideration here, this is not of importance, since we are dealing with a surface boundary layer to which the influence of the bottom boundary layer is not extended.

After rearranging all variables at time step $t+1$ to the left-hand side, we obtain the matrix equation

$$[c1_k]\varphi_{k-1}^{t+1} + [c2_k]\varphi_k^{t+1} + [c3_k]\varphi_{k+1}^{t+1} = [c4_k], \tag{16}$$

which is solved by means of standard Gaussian elimination and back substitution. Here $\varphi = (w, b)$ and the coefficients of the matrix equation (16) are, for $\varphi = w$,

$$c1_k = -\frac{2\theta_2 \Delta t}{\Delta z_{k+1} + \Delta z_k} \frac{v_k}{\Delta z_k},$$

$$c2_k = 1 + \theta_1 \mathrm{i}\alpha + \frac{2\theta_2 \Delta t}{\Delta z_{k+1} + \Delta z_k} \left(\frac{v_k}{\Delta z_k} + \frac{v_{k+1}}{\Delta z_{k+1}} \right),$$

$$c3_k = \frac{2\theta_2 \Delta t}{\Delta z_{k+1} + \Delta z_k} \frac{v_{k+1}}{\Delta z_{k+1}},$$

$$c4_k = [1 - (1-\theta_1)\mathrm{i}\alpha] w_k^t + \Delta t p^t + \frac{2(1-\theta_2)\Delta t}{\Delta z_{k+1} + \Delta z_k} \left(v_{k+1} \frac{w_{k+1}^t - w_k^t}{\Delta z_{k+1}} - v_k \frac{w_k^t - w_{k-1}^t}{\Delta z_k} \right)$$

and for $\varphi = b$,

$$c1_k = -\frac{\alpha_b \theta_2 \Delta t}{\Delta z_k} \frac{v_k + v_{k-1}}{\Delta z_k + \Delta z_{k-1}},$$

$$c2_k = 1 + \frac{\alpha_b \theta_2 \Delta t}{\Delta z_k} \left(\frac{v_{k+1} + v_k}{\Delta z_{k+1} + \Delta z_k} + \frac{v_k + v_{k-1}}{\Delta z_k + \Delta z_{k-1}} \right) + \frac{2\theta_4 \Delta t c_0^4}{v_k} b_k^t,$$

$$c3_k = -\frac{\alpha_b \theta_2 \Delta t}{\Delta z_k} \frac{v_{k+1} + v_k}{\Delta z_{k+1} + \Delta z_k},$$

$$c4_k = \left(1 - \frac{\Delta t c_0^4}{v_k} (1 - 2\theta_4) b_k^t \right) b_k^t + \frac{\alpha_b (1 - \theta_2) \Delta t}{\Delta z_k} \left((v_{k+1} + v_k) \frac{b_{k+1}^t - b_k^t}{\Delta z_{k+1} + \Delta z_k} - (v_k + v_{k-1}) \frac{b_k^t - b_{k-1}^t}{\Delta z_k + \Delta z_{k-1}} \right)$$

$$+ v_k \begin{cases} \theta_3 \left[\left(\frac{u_k^{t+1} - u_{k-1}^{t+1}}{\Delta z_k} \right)^2 + \left(\frac{v_k^{t+1} - v_{k-1}^{t+1}}{\Delta z_k} \right)^2 \right] + (1 - \theta_3) \left[\left(\frac{u_k^t - u_{k-1}^t}{\Delta z_k} \right)^2 + \left(\frac{v_k^t - v_{k-1}^t}{\Delta z_k} \right)^2 \right] \\ \qquad \text{(for expression (8))} \\ \left[\left(\theta_3 \frac{u_k^{t+1} - u_{k-1}^{t+1}}{\Delta z_k} + (1 - \theta_3) \frac{u_k^t - u_{k-1}^t}{\Delta z_k} \right)^2 + \left(\theta_3 \frac{v_k^{t+1} - v_{k-1}^{t+1}}{\Delta z_k} + (1 - \theta_3) \frac{v_k^t - v_{k-1}^t}{\Delta z_k} \right)^2 \right] \\ \qquad \text{(for expression (9))} \end{cases}$$

The equations are solved in the following sequence: first the solution of the equation for the complex velocity is found, from which the *u*- and the *v*-velocity are determined; then the equation for the turbulent kinetic energy is solved and thereafter the eddy viscosity is computed. In this sequence the computations are performed at each time step.

At this point it is important to stress that even though in this context an approximation is called implicit or semi-implicit, it is not strictly the case because it involves an eddy viscosity which is taken from the previous time step. In order to remedy this contradiction, an iterative procedure for the eddy viscosity coefficient may be applied. Whenever the iterative procedure is employed, as discussed in the following section, convergence is considered to be attained if the relative discrepancy between 'old' and 'new' eddy viscosities does not exceed 1 per cent.

4. NUMERICAL EXPERIMENTS

A series of numerical experiments was set up with the aim of understanding the causes leading to the appearance of spikes and jittering. With this aim in mind, all possible combinations of explicit, implicit and semi-implicit approximations for the various terms in the model equations were tested, the exception being the Coriolis term which was approximated by either an implicit or a semi-implicit scheme only to overcome the drastic time step limitation as imposed by the criteria of stability.

By making use of the model described above, we simulated the evolution of the neutrally stratified upper Ekman boundary layer forced by a constant wind stress. The water depth was taken to be 100 m, deep enough to eliminate the influence of the bottom boundary layer on the surface boundary layer, a wind stress of 0·1 N m^{-2} along the *y*-axis was applied, following Eifler and Schrimpf,[15] the limiting value of the mixing length L_0 was set to 2·5 m, the latitude was specified to be 30°N and a total run of 100 days was chosen in order to reach, or at least approach, steady state, unless specified otherwise, a constant grid spacing $\Delta z = 1{\cdot}0$ m was used.

In Figure 1, the complete set of numerical experiments which were performed is depicted. Here the symbol 'f' denotes the Coriolis term, 'D' the vertical diffusion of momentum and turbulent kinetic

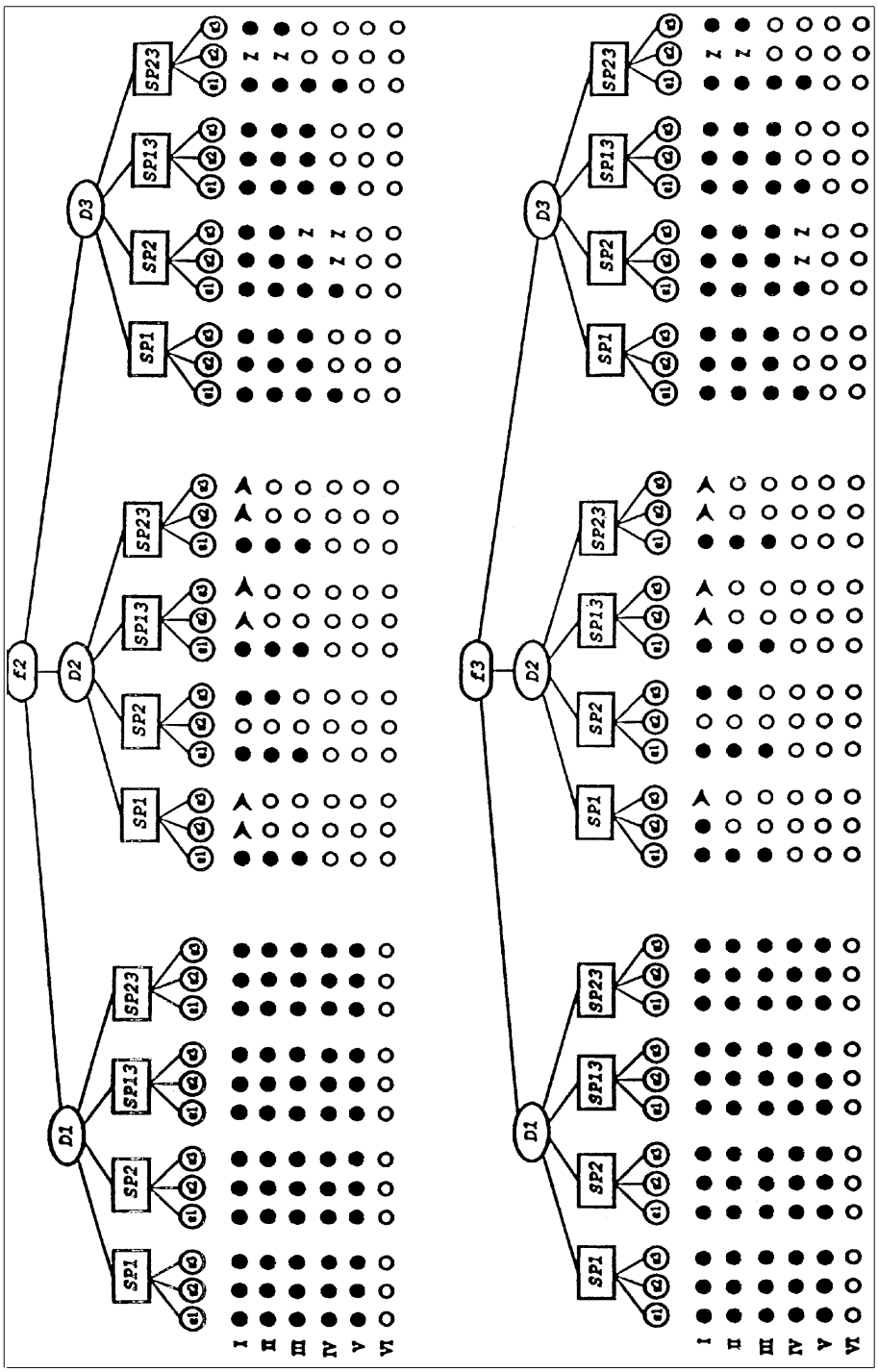

Figure 1. Set of numerical experiments and properties of solution obtained when using different combinations of approximations for various terms of model equations. Terms: f, Coriolis term; D, vertical turbulent diffusion of momentum and turbulent kinetic energy; SP, shear production; ε, dissipation of turbulent kinetic energy. Approximations: 1, explicit; 2, implicit; 3, semi-implicit. Time steps: I, $\Delta t = 1$ h; II, $\Delta t = 30$ min; III, $\Delta t = 15$ min; IV, $\Delta t = 5$ min; V, $\Delta t = 1$ min; VI, $\Delta t = 30$ s. Properties: ○, stable solution; ●, unstable solution; ➤, spikes; z, jittering

energy, 'SP' the shear production (recall that SP1 and SP2 are defined by (10) and (11)) and 'ε' the dissipation of turbulent kinetic energy. The numbers 1, 2 and 3 denote respectively that an explicit, an implicit or a semi-implicit approximation was used. For example, 'SP2.3' means that a semi-implicit approximation for the shear production term SP2 was employed. An open circle indicates that a stable solution was obtained, a full circle means that the solution 'exploded' owing to numerical instability, the symbol '>' indicates that spikes were observed and the symbol 'z' shows where jittering was detected. The computations were carried out with time step $\Delta t = 1$ h for row I, $\Delta t = 30$ min for row II, $\Delta t = 15$ min for row III, $\Delta t = 5$ min for row IV, $\Delta t = 1$ min for row V and $\Delta t = 30$ s for row VI. All in all, 72 combinations of approximations are possible for a given time step and a given vertical resolution.

As can be seen from Figure 1, spikes only occur if we use (i) a time step $\Delta t = 1$ h and (ii) an implicit approximation for the D-term. The only combinations of approximations which do not show spikes even though both conditions (i) and (ii) are satisfied are f2–D2–SP2–ε2 and f3–D2–SP2–ε2, i.e. those combinations which employ implicit approximations for each of the terms in the turbulent kinetic energy equation. On the other hand, jittering is observed for a range of different time steps ($\Delta t = 1$ h to $\Delta t = 5$ min), but only when making use of a semi-implicit approximation for the D-term and combinations of the form I–f2–SP2.3–ε2, II–f2–SP2.3–ε2, III–f2–SP2–ε3, IV–f2–SP2–ε2 and IV–f2–SP2–ε3, as well as if a semi-implicit approximation for the Coriolis term and combinations of the form I–SP2.3–ε2, II–SP2.3–ε2, IV–SP2–ε2, IV–SP2–ε3 are employed.

It can also be deduced from Figure 1 that it is the choice of approximation for the vertical turbulent diffusion term which determines the maximum possible time step for the solution to be free of any numerical artefacts. This time step turns out to be 30 s for D1, 1 min for D3 and 5 min for D2. Not surprisingly, the greatest time step can be employed with an implicit approximation for the vertical diffusion term, regardless of which approximations, or any combination thereof, are chosen for the shear production, dissipation and Coriolis terms. Comparing the solutions obtained with an implicit or a semi-implicit approximation for the D-term, i.e. D2 or D3, also shows that more combinations involving D2 produce stable solutions regardless of which approximation for the Coriolis term is used.

Spikes

The vertical distributions of different characteristics, given the combination of the form I–f3–D2–SP1.3–ε2, are shown in Figure 2 (note that the horizontal scales in Figures 2–5 may vary). The influence of changing the vertical resolution is illustrated by comparison of Figures 2(a)–2(d) and 2(e)–2(h), which correspond to $\Delta z = 1{\cdot}0$ and $0{\cdot}5$ m respectively.

We see that spikes occur at the base of the surface boundary layer. They appear in the profiles of the momentum flux $\nu|\partial w/\partial z|$ (Figures 2(b) and 2(f)) and the components of the turbulent kinetic energy budget (Figures 2(c) and 2(g)) and the turbulent kinetic energy b (Figures 2(d) and 2(h)) and manifest themselves as step-like discontinuities in the vertical profiles of the mean u- and v-velocity (Figures 2(a) and 2(e)). It is readily seen that spikes are drastically enhanced when using a finer vertical resolution. Not surprisingly, the solution with an even finer resolution, $\Delta z = 0{\cdot}2$ m, 'exploded' and would require a reduction of the time step for the solution to be stable. An important point to note is that spikes are only observed during the period of a deepening surface boundary layer and disappear when the lower boundary of this layer reaches the seabed. Their lifetime is of the order of a few days, depending on the external parameters.

The answer to the question of whether the discontinuities in the velocity profiles lead to the artificially high shear and hence to unrealistic production of turbulent kinetic energy or whether the spikes in the turbulent characteristics give rise to those discontinuities is of no importance. There is

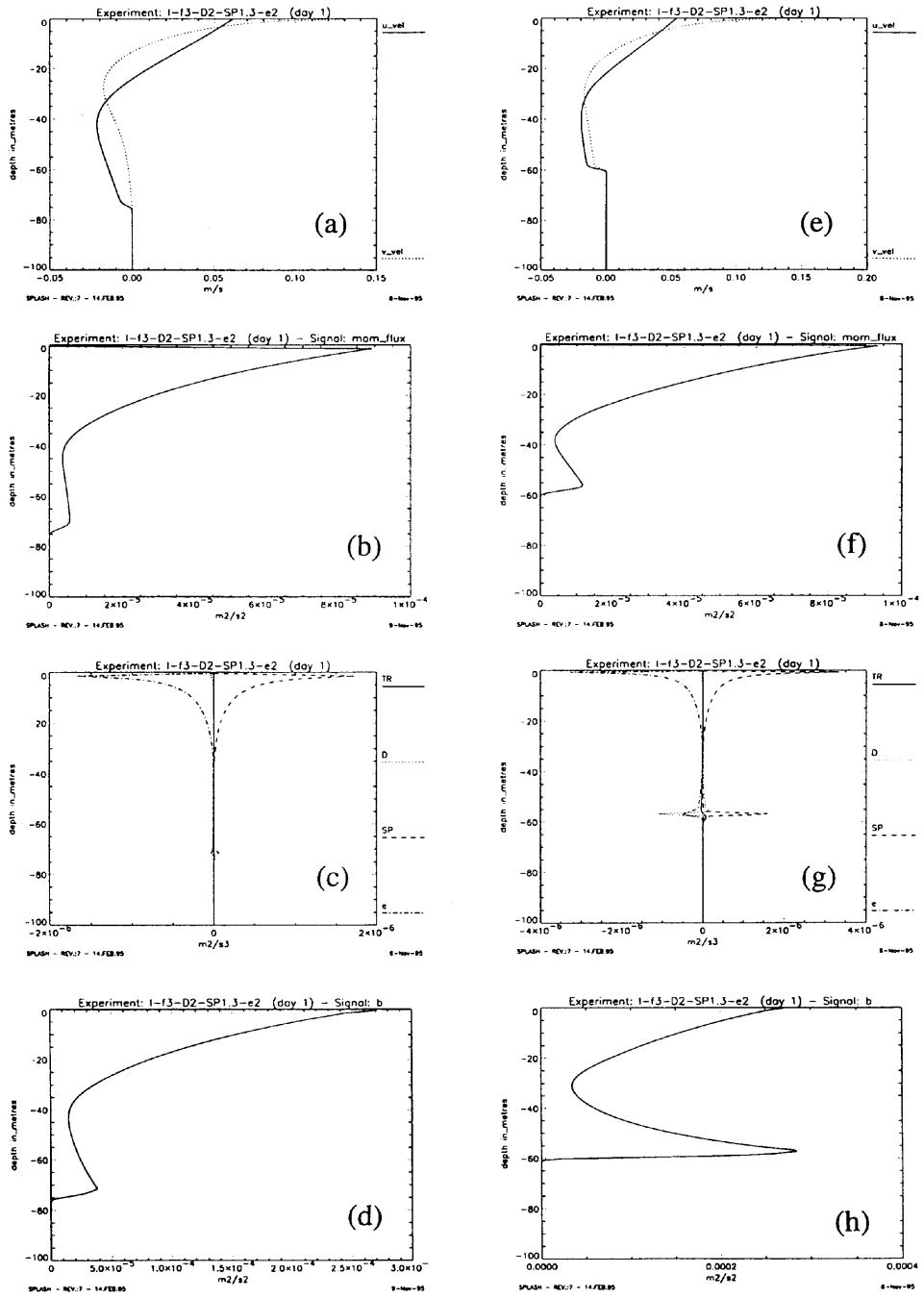

Figure 2. Spikes at base of surface planetary boundary layer, obtained after 1 day of simulation with combination I–f3–D2–SP1.3–e2 and (a)–(d) $\Delta z = 1{\cdot}0$ m; (e)–(h) $\Delta z = 0{\cdot}5$ m: (a), (e) mean u- and v-velocity; (c), (g) components of turbulent kinetic energy equation; (b), (f) momentum flux; (d), (h) turbulent kinetic energy. (TR, temporal rate of change; D, vertical diffusion; SP, shear production; e, turbulent kinetic energy dissipation). Note variable horizontal scales

reason to believe that an inadequate numerical description of the non-linear interaction between turbulence and mean velocity due to an inappropriate choice of combination of approximations and large time steps Δt is responsible for this type of numerical artefact. The only combinations which produce stable solutions devoid of any spikes at $\Delta t = 1$ h are those which employ implicit approximations consistently for all the terms of the turbulent kinetic energy equation. It was also found that making use of the iterative procedure for the eddy viscosity, as described in Section 3, removed the spikes in all the cases in which they were previously obtained.

Jittering

Jittering in the vertical profiles of the various characteristics, obtained with combinations of the form I–f2–D3–SP2.3–ε2, IV–f2–D3–SP2–ε2 and IV–f2–D3–SP2–ε3, is illustrated in Figures 3 and 4. Analysis of these figures reveals the presence of transient and permanent jittering.

Transient jittering occurs during the spin-up period. For the case presented in Figure 3, this peculiarity has a lifetime of 1 week. Shown in Figures 3(a)–3(d) are the vertical profiles of the mean u- and v-velocity, the momentum flux and the components of the turbulent kinetic energy budget and the turbulent kinetic energy after 1 day of simulation. It can be seen that strong jittering disturbs each of the profiles of the mean velocity and turbulence characteristics throughout the entire surface boundary layer. The same profiles after 5 days of simulation are depicted in Figures 3(e)–3(h), where jittering is completely damped out in the vertical profiles of all the characteristics, except for the momentum flux, in which small zigzag changes are still observable. However, after 7 days of simulation these disturbances also disappear and the solution is totally free of any peculiarities. This is an illustration of the fact that transient jittering persists longest in the vertical profiles of the momentum flux. When employing a finer vertical resolution ($\Delta z = 0{\cdot}5$ m), transient jittering with a lifetime of several days is observed at time step $\Delta t = 15$ min. Introducing the iterative procedure for the eddy viscosity does not eliminate transient jittering, though the amplitude of jittering is reduced.

Permanent jittering is illustrated in Figure 4, where this feature is detected either in the turbulence characteristics only, shown here for the combination of the form IV–f2–D3–SP2–ε2 (Figures 4(a)–4(d)), or in both the mean velocity and turbulence characteristics, shown in Figures 4(e)–4(h) for the combination of the form IV–f2–D3–SP2–ε3. The vertical profiles depicted were obtained after 500 days of simulation in which jittering remained unchanged during the period 50–500 days. It was still present after 1000 days and hence can be considered as a permanent artefact. A curiosity is that while the use of an implicit approximation for all the terms guarantees the lack of any jittering at all time steps, a semi-implicit scheme for the D-term introduces jittering at the relatively small time step $\Delta t = 5$ min. In fact, permanent jittering is observed at moderate time steps only. Figures 4(b)–4(d) illustrate its manifestation in the turbulence characteristic and momentum flux profiles. From these figures we notice that the magnitude of jittering is apparently less than a certain threshold value, so this feature is not detectable in the profiles of the mean velocity (Figure 4(a)). Another change in the approximation, from an implicit scheme for the ε-term to a semi-implicit one, without changing any of the other model parameters, leads to larger jittering which, correspondingly, is also observable in the mean velocity profiles (Figure 4(e)). Comparing the vertical profiles of the various components of the turbulent kinetic energy budget (Figures 4(c) and 4(d)) provides us with some new information. Although the approximation ε2 is changed to ε3, the dissipation profile is not substantially affected. Larger jittering is present only in the temporal rate of change and shear production of turbulent kinetic energy, whereas the influence of the vertical turbulent kinetic energy diffusion is almost negligible.

In order to understand the causes leading to the appearance of jittering, we verified the validity of the criterion $\Delta t_{\text{crit}} \geqslant 2(\Delta z)^2/\max(\nu)$ for the existence of this phenomenon, which has been put

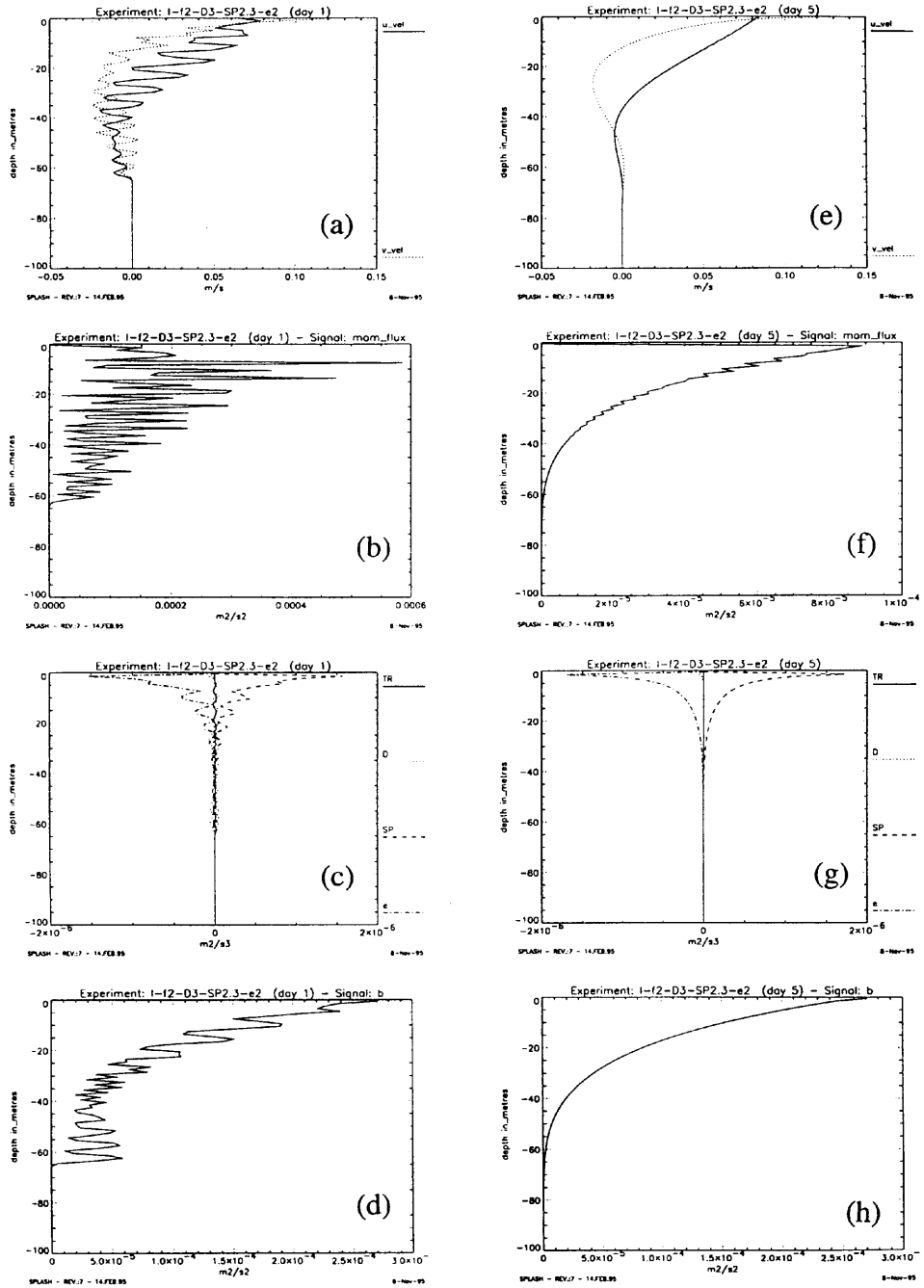

Figure 3. Transient jittering occurring during spin-up period: (a)–(d) profiles of mean velocity and turbulence characteristics after 1 day and (e)–(h) after 5 days of simulation with combination I–f2–D3–SP2.3–e2. Note variable horizontal scales

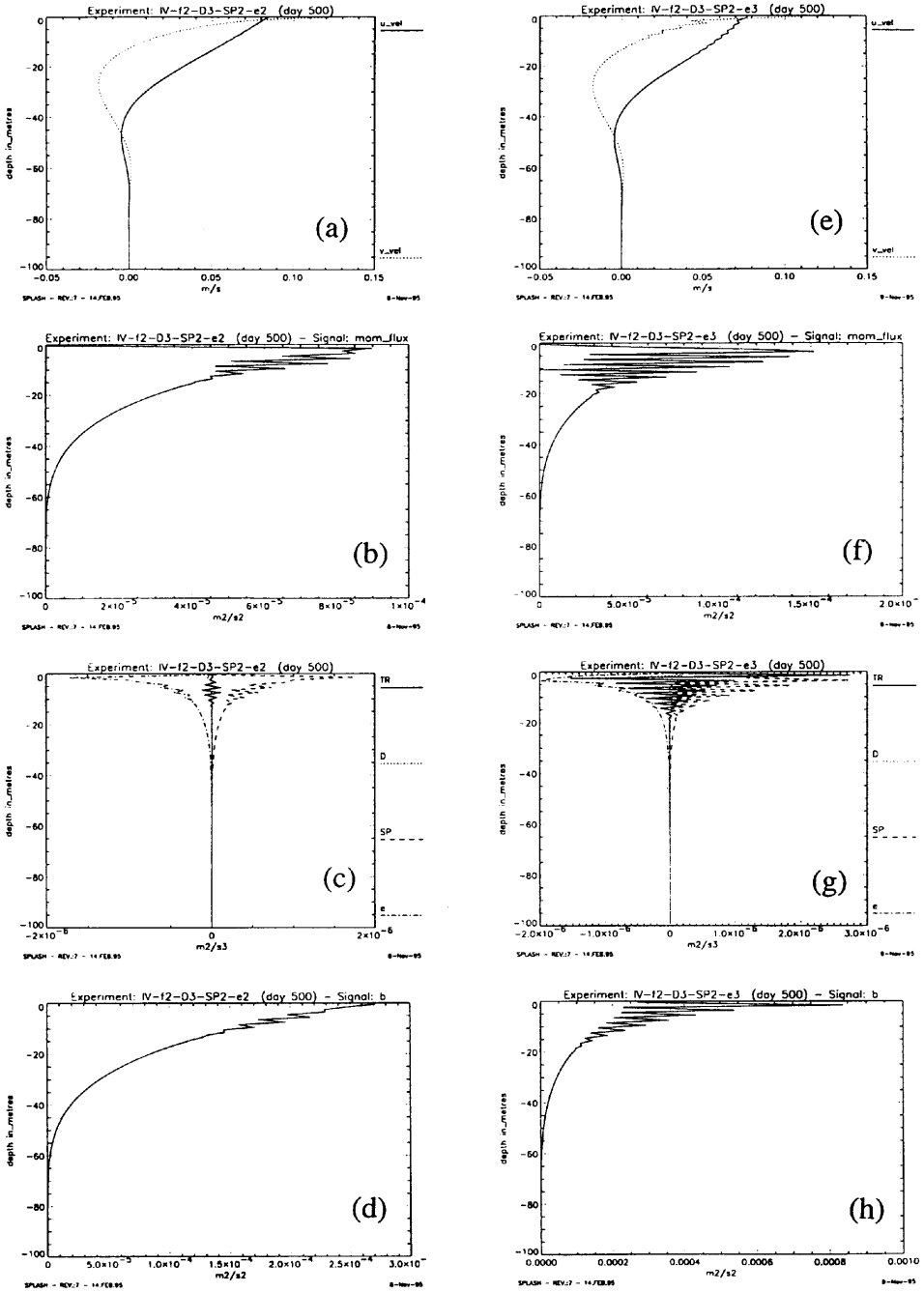

Figure 4. Permanent jittering after 500 days of simulation with combination IV–f2–D3–SP2: (a)–(d) jittering observable in turbulence characteristics only when using implicit dissipation (e2); (e)–(h) jittering in both mean velocity and turbulence characteristics when using semi-implicit dissipation (e3). Note variable horizontal scales

forward by Frey,[1] in analogy with the stability criterion for a one-dimensional heat conductivity problem with constant heat diffusivity. It was found that for every occurrence of jittering as indicated in Figure 1, the criterion was exceeded. For example, when using the combination of the form f2–D3–SP2–ε2 with $\Delta t = 300$ s and $\Delta z = 1{\cdot}0$ m, the above criterion for $\max(v) = 0{\cdot}0115$ m^2 s^{-1} indicates that jittering occurs for $\Delta t_{\text{crit}} > 174$ s, which is clearly the case. It is important to note that with a reduction in time step to $\Delta t = 200$ s (with the corresponding values of Δt_{crit} and $\max(v)$ being 174 s and $0{\cdot}0115$ m^2 s^{-1} respectively), jittering is removed even though the critical time step is exceeded. Moreover, experiments with finer vertical resolutions, $\Delta z = 0{\cdot}5$ m and $\Delta z = 0{\cdot}25$ m, confirm that jittering is absent even though the time step was chosen to be greater than the critical one. These findings show that for the combinations which give rise to jittering, the criterion is a necessary though rather crude condition for the existence of this peculiarity. However, as can be seen from Figure 1, there are other combinations for which jittering does not occur even if the criterion is exceeded. In this sense the proposed criterion is an insufficient condition for the existence of jittering. Employing the iterative procedure for the eddy viscosity eliminated the phenomenon of permanent jittering in all the cases in which it was previously obtained.

It was also found that, upon progressively increasing the time step, the transition from a stable to an unstable solution happened in two different ways. On one hand, there is a *sudden transition* without jittering from a stable solution at $\Delta t = 368{\cdot}5$ s to an unstable one when the time step increases by only $0{\cdot}1$ s; this was observed in the experiment labelled f3–D2–SP1.3–ε1. On the other hand, there is also a *gradual transition* when jittering occurs during the entire transition period. This behaviour, depicted in Figure 5, showing the details of the surface boundary layer only (down to a depth of 50 m), was detected when using the combination of the form f2–D3–SP2–ε1. From Figure 1 it follows that this combination ensures a stable solution at $\Delta t = 1$ min and 'explodes' at $\Delta t = 5$ min. Successively increasing the time step, starting from the stable solution, reveals (Figures 5(a)–5(c)) that $\Delta t = 131$ s is the maximum possible time step for the solution to remain stable. At $\Delta t = 132$ s, jittering is small, but it grows in magnitude upon further increasing the time step. The results of this can be seen in Figure 5(d), depicting the components of the v-momentum equation (recall that wind forcing is applied in the y-direction). We notice that jittering affects the temporal rate of change in v-velocity and the vertical diffusion of influx. Jittering is observable in the $\partial b/\partial t$-term (Figure 5(e)) but is hardly discernible in the b-profile (Figure 5(f)). Maximum jittering is obtained with $\Delta t = 141$ s (Figures 5(g)–5(i)). It now affects the shear production and dissipation (Figure 5(h)) and hence also the turbulent kinetic energy (Figure 5(i)). Eventually, at $\Delta t = 142$ s the solution becomes unstable. Gradual transition to instability through jittering was observed in several other cases when using combinations of D3-type.

These results testify that jittering can serve as a herald of instability, although a sudden transition from a stable to an unstable solution can also occur. It is thus evident that Figure 1 cannot be regarded as being complete. In fact, if the whole range of time steps from 1 h to 30 s could have been displayed in, say, 1 s intervals, we could observe that there are more cases of gradual transitions than are shown in Figure 1.

We can summarize that the phenomena of spikes and jittering are not only the result of violating stability conditions owing to an inconsistent choice of temporal and vertical resolutions, but also of inappropriate approximations for the turbulent kinetic energy equation. It is precisely these reasons which lead to numerical instability and hence to such drastic consequences as spikes and jittering which distort, if not entirely corrupt, the solution. This is confirmed by the fact that the consistent use of implicit approximations does not produce these phenomena. We also demonstrated that the iterative procedure for the eddy viscosity eliminates spikes and permanent jittering but does not remove transient jittering, though the magnitude of the latter is reduced.

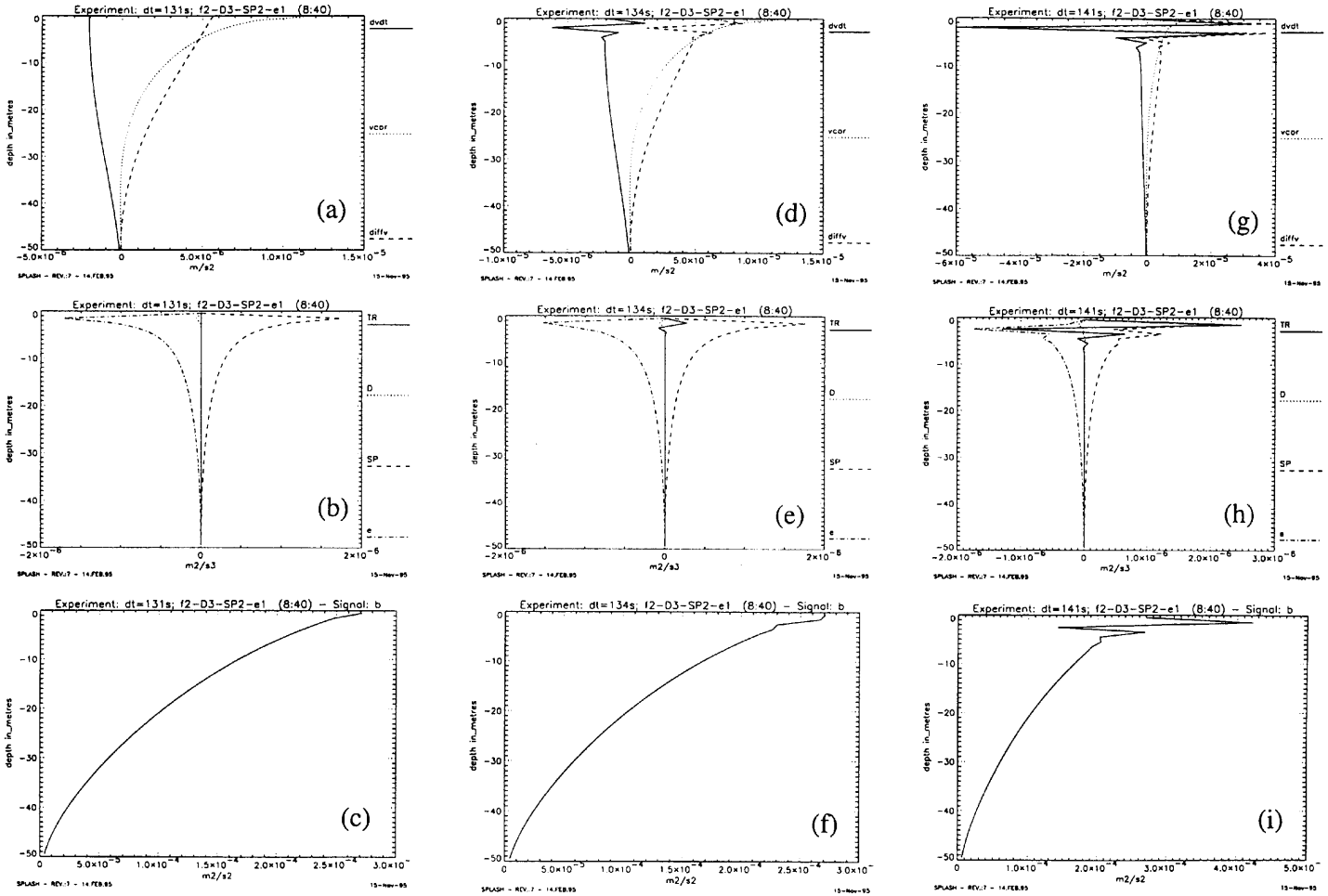

Figure 5. Gradual transition via jittering to instability obtained with combination f2–D3–SP2–e1 and (a)–(c) $\Delta t = 131$ s; (d)–(f) $\Delta t = 134$ s; (g)–(i) $\Delta t = 141$ s: (a), (d), (g) components of v-momentum equation (dvdt, temporal rate of change; vcor, Coriolis term; diffv, vertical diffusion of v-momentum); (b), (e), (h) components of turbulent kinetic energy equation; (c), (f), (i) turbulent kinetic energy. Note variable horizontal scales; the vertical scale is taken to be 50 m to show the surface planetary boundary layer only

5. CONCLUSIONS

Whilst spikes and jittering in the vertical profiles of mean velocity and turbulence characteristics have been observed by several authors, the explanations of their causes and how to avoid these numerical artefacts remain rather contradictory. In order to answer these questions, a series of numerical experiments was set up with all possible combinations of explicit, implicit and semi-implicit approximations for the equations of a simple *b–L* planetary boundary layer model. As a test case the neutrally stratified surface Ekman boundary layer forced by a constant wind stress was considered.

Analysis of the results obtained leads to the following findings. Spikes are only detected if an implicit approximation for the vertical diffusion term and large time steps are used. This feature occurs at the base of the boundary layer and has a lifetime or the order of several days. Jittering is observable throughout the entire boundary layer depth and reveals itself when employing a semi-implicit approximation for the vertical diffusion term over a wide range of time steps. Two types of jittering are distinguishable: transient and permanent. The former occurs during the spin-up period and has a lifetime of about 1 week. This feature persists longest in the momentum flux profile. Permanent jittering, on the other hand, has a lifetime of more than 1000 days and is detected either in the turbulence characteristics only or in both the mean velocity and turbulence characteristics. It is also noted that the transition from a stable solution to an unstable one can happen suddenly or gradually. In the first case, jittering is absent; in the second case, jittering is observed during the entire transition period. This behaviour can serve as testimony to the fact that jittering is a herald of instability.

The study shows that for jittering to occur, the empirical criterion proposed by Frey[1] is a necessary though insufficient condition. The existence of spikes or jittering depends, among other things, on the choice of approximations for the different terms in the turbulent kinetic energy equation. That is, spikes and jittering are obtained with certain combinations of approximations only and can be avoided when using different ones. We thus conclude that spikes and jittering may be regarded as artefacts caused by numerical instability. A combination which employs implicit approximations consistently for all the terms in the turbulent kinetic energy equation, regardless of whether an implicit or a semi-implicit approximation for the Coriolis term is used, proves to devoid of any numerical artefacts over the whole range of time steps considered. It is further found that by introducing an iterative procedure for the eddy viscosity, spikes and permanent jittering are removed owing to apparently minimizing an imbalance in the turbulent kinetic energy budget which is caused by taking the eddy viscosity from the previous time step.

Finally, it has to be stressed that we only considered the simplest test case imaginable. It seems likely that in realistic situations, with fluctuating wind stress and/or buoyancy flux at the sea surface, the effects of spikes and jittering may distort the solution throughout the entire simulation period if precautions are not taken. Moreover, these effects may not be distinguishable from their natural variability. It follows that it is of the utmost importance to eliminate any possibility for these phenomena to appear.

ACKNOWLEDGEMENTS

This work was carried out during a stay of B. A. Kagan as visiting scientist at the Joint Research Centre, Ispra. A. G. Pufahl is funded by a European Community grant under the Human Mobility and Capital programme. The authors are indebted to Dr. R. Proctor, Dr. A. M. Davies and an anonymous reviewer for their valuable remarks and W. Hammans for preparing the diagrams.

REFERENCES

1. H. Frey, 'A three-dimensional, baroclinic shelf–sea circulation model. 1. The turbulence closure scheme and the one-dimensional test model', *Cont. Shelf Res.*, **11**, 365–395 (1991).

2. G. L. Mellor and T. Yamada, 'A hierarchy of turbulence closure models for planetary boundary layers', *J. Atmos. Sci.*, **31**, 1791–1806 (1974).
3. G. L. Mellor and T. Yamada, 'Development of a turbulence closure model for geophysical fluid problems', *Rev. Geophys. Space Phys.*, **20**, 851–875 (1982).
4. A. M. Davies and J. E. Jones, 'On the numerical solution of the turbulence energy equations for wave and tidal flows', *Int. j. numer. methods fluids*, **12**, 17–41 (1991).
5. ASCE Task Committee on Turbulence Models in Hydraulic Computations, 'Turbulence modeling of surface water flow and transport', *J. Hydraul. Eng.*, **114**, 969–1152 (1988).
6. W. Rodi, 'Turbulence models and their application in hydraulics—a state of the art review', *Sonderforschungsbereich 80*, University of Karlsruhe, 1980.
7. B. E. Launder and D. B. Spalding, *Mathematical Models of Turbulence*, Academic, London, 1972.
8. E. Deleersnijder and P. Luyten, 'On the practical advantages of the quasi-equilibrium version of the Mellor and Yamada level 2·5 turbulence closure applied to marine modelling', *J. Appl. Math. Model.*, **18**, 281–287 (1994).
9. A. M. Davies, P. J. Luyten and E. Deleersnijder, 'Turbulence energy models in shallow sea oceanography', in *Quantitative Skill Assessment for Coastal Ocean Models*, CES Vol. 47, 1995, pp. 97–123.
10. H. Burchard and H. Baumert, 'On the performance of a mixed-layer model based on the k–ε turbulence closure', *J. Geophys. Res.*, **100**, 8523–8540 (1995).
11. K. C. Duwe, R. R. Hewer and J. O. Backhaus, 'Results of a semi-implicit two-step method for the simulation of markedly nonlinear flow in coastal seas', *Cont. Shelf Res.*, **2**, 255–274 (1983).
12. B. Galperin, L. Kantha, S. Hassid and A. Rosati, 'A quasi-equilibrium turbulent energy model for geophysical flows', *J. Atmos. Sci.*, **45**, 55–62 (1988).
13. A. K. Blackadar, 'The vertical exchange distribution of wind and turbulent exchange in a neutral atmosphere', *J. Geophys. Res.*, **67**, 3095–3102 (1962).
14. S. S. Zilitinkevich, D. L. Laikhtman and A. S. Monin, 'Dynamics of the atmospheric boundary layer', *Izv. AN SSSR*, *Fiz. Atmos. Okeana*, **3**, 287–333 (1967).
15. W. Eifler and W. Schrimpf, 'Ispramix—a hydrodynamic program for computing regional sea circulation patterns and transfer processes', *JRC Rep. EUR14856*, Ispra, 1992.

